Employing the geostrophic ($fv_g = \partial\phi/\partial x$ and $-fu_g = \partial\phi/\partial y$) and the hydrostatic ($\partial\phi/\partial p = -RT/p$) relationships, this can be expressed as

$$DEF = -\frac{2}{f}\left[J\left(fv_g, -\frac{R}{p}\frac{\partial T}{\partial x}\right) + J\left(-fu_g, -\frac{R}{p}\frac{\partial T}{\partial y}\right)\right]$$

or

$$DEF = \frac{2R}{p}\left[J\left(v_g, \frac{\partial T}{\partial x}\right) - J\left(u_g, \frac{\partial T}{\partial y}\right)\right]. \tag{6.33b}$$

Carrying out the indicated derivatives and then grouping like terms together yields

$$DEF = \frac{2R}{p}\left[\left(\frac{\partial v_g}{\partial x} + \frac{\partial u_g}{\partial y}\right)\frac{\partial^2 T}{\partial x \partial y} - \frac{\partial v_g}{\partial y}\frac{\partial^2 T}{\partial x^2} - \frac{\partial u_g}{\partial x}\frac{\partial^2 T}{\partial y^2}\right]. \tag{6.33c}$$

Denoting the geostrophic shearing deformation, $(\partial v_g/\partial x + \partial u_g/\partial y)$, as SH, the geostrophic stretching deformation, $(\partial u_g/\partial x - \partial v_g/\partial y)$, as ST, and employing the non-divergence of the geostrophic wind, (6.33c) can be rewritten as

$$DEF = \frac{2R}{P}\left[(SH)\frac{\partial^2 T}{\partial x \partial y} + \frac{(ST)}{2}\left(\frac{\partial^2 T}{\partial x^2} - \frac{\partial^2 T}{\partial y^2}\right)\right] \tag{6.33d}$$

which illustrates that the deformation terms will be significant where second derivatives of temperature are coincident with deformation (i.e. first derivatives) in the geostrophic wind field. Mid-latitude frontal regions, as we will see, are defined by such conditions. This fact has led to the historical assumption that the deformation term is only large in frontal regions. As it turns out, a number of other recurrent but non-frontal thermal structures in mid-latitude cyclones are also characterized by these conditions – most notably the large-scale thermal ridge often associated with occluded cyclones. From this perspective, neglect of the deformation term is liable to lead to significant misdiagnosis in many canonical mid-latitude cyclone environments (as we will show later). Next we will derive an alternative expression for the forcing for quasi-geostrophic vertical motions that includes these terms, lends additional insight into the nature of the mid-latitude atmosphere, and is amenable to simple graphical evaluation.

6.4 The $\vec{Q}$-Vector

The remainder of this chapter will be devoted to examining the so-called $\vec{Q}$-vector form of the quasi-geostrophic omega equation introduced by Hoskins *et al.* (1978). Consideration of the $\vec{Q}$-vector reveals an unexpected and intriguing characteristic of the thermal wind balance that will serve as a cornerstone in the development of a deeper conceptual understanding of the nature of quasi-geostrophic vertical motions. We begin by investigating the geostrophic paradox.

6.4.1 The geostrophic paradox and its resolution

Consider the jet entrance region depicted in Figure 6.8. The confluent, geostrophic wind field depicted there acts to tighten the horizontal temperature gradient at C. Any such increase in the magnitude of the temperature gradient forces an increase in the geostrophic vertical shear via the thermal wind relationship. Simultaneously, the geostrophic wind advects lower geostrophic momentum (quantified by the isotachs of the y-direction geostrophic wind) into the jet core. The momentum advection tends to decrease the wind speed at C and, thus, contributes to a decrease in the vertical shear of the geostrophic wind in that column. Thus, the very same geostrophic flow that serves to increase the magnitude of the horizontal temperature gradient at C also serves to decrease the vertical shear of the geostrophic wind at C via negative geostrophic momentum advection. This set of circumstances presents a paradox: that is, on the one hand, geostrophic temperature advection should increase the thermal wind at C and, on the other, geostrophic momentum advection should decrease it at C. So, the geostrophic wind actually destroys thermal wind balance by affecting opposite signed changes to the two components of that balance. Since the thermal wind balance is a form of the geostrophic balance, it can therefore be said that the geostrophic wind destroys itself! We will refer to this property of the geostrophic flow as the geostrophic paradox.

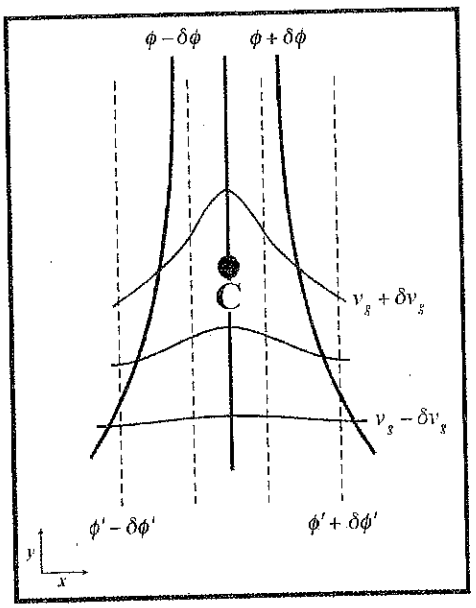

Figure 6.8 Jet entrance region in the northern hemisphere. Thick solid lines are 500 hPa geopotential height, dashed lines are 1000–500 hPa thickness, and thin solid lines are isotachs of the y-direction geostrophic wind. Point C is mentioned in the explanation given in the text

Interestingly, however, observations suggest that the synoptic-scale flow in the middle latitudes is very nearly in geostrophic balance at all times. How can this be in the face of what we have just described? There must be another portion of the flow that acts to maintain the geostrophic balance in the face of its self-destructive tendency. That portion of the flow is the forced, ageostrophic, secondary circulation.[5] Since the geostrophic flow tends to create thermal wind imbalance, the forced secondary circulation must bring the flow back toward a state of geostrophic balance. This may be accomplished if the secondary circulation counteracts the tendencies induced by the geostrophic wind itself. Therefore, the secondary, ageostrophic circulation operating in the vicinity of the jet entrance region depicted in Figure 6.8 must simultaneously (1) decrease the magnitude of the horizontal temperature gradient, and (2) increase the vertical shear. We now examine a derivation that quantifies the geostrophic paradox and in so doing leads to a description of the forced, secondary circulation that resolves it.

We begin by considering both the thermodynamic energy equation and the y equation of motion at the level of quasi-geostrophic theory:

$$\left(\frac{\partial}{\partial t} + \vec{V}_g \cdot \nabla\right) v_g + f_0 u_{ag} = 0 \quad \text{and} \quad \left(\frac{\partial}{\partial t} + \vec{V}_g \cdot \nabla\right)\left(-\frac{\partial \phi}{\partial p}\right) - \sigma\omega = 0.$$

Neglecting the ageostrophy for the moment, these expressions can be rewritten as

$$\left(\frac{\partial}{\partial t} + \vec{V}_g \cdot \nabla\right) v_g = 0 \tag{6.34a}$$

and

$$\left(\frac{\partial}{\partial t} + \vec{V}_g \cdot \nabla\right)\left(-\frac{\partial \phi}{\partial p}\right) = 0. \tag{6.35a}$$

Recall that the thermal wind balance for the situation depicted in Figure 6.8 is given by

$$f_0 \frac{\partial v_g}{\partial p} = \frac{\partial^2 \phi}{\partial x \partial p}.$$

Now, $f_0 \partial/\partial p$ of (6.34a) is equal to

$$\begin{aligned} f_0 \frac{\partial}{\partial p}\left[\left(\frac{\partial}{\partial t} + \vec{V}_g \cdot \nabla\right) v_g\right] &= f_0 \frac{\partial}{\partial p}\left[\frac{\partial v_g}{\partial t} + u_g \frac{\partial v_g}{\partial x} + v_g \frac{\partial v_g}{\partial y}\right] \\ &= \left(\frac{\partial}{\partial t} + \vec{V}_g \cdot \nabla\right)\left(f_0 \frac{\partial v_g}{\partial p}\right) \\ &\quad + f_0\left[\frac{\partial u_g}{\partial p}\frac{\partial v_g}{\partial x} + \frac{\partial v_g}{\partial p}\frac{\partial v_g}{\partial y}\right]. \end{aligned}$$

[5] This flow is referred to as 'secondary' in order to distinguish it from the primary, geostrophic flow.

Employing the thermal wind relationship and the non-divergence of the geostrophic wind, this can be rewritten as

$$f_0 \frac{\partial}{\partial p}\left[\left(\frac{\partial}{\partial t}+\vec{V}_g\cdot\nabla\right)v_g\right]=\left(\frac{\partial}{\partial t}+\vec{V}_g\cdot\nabla\right)\left(f_0\frac{\partial v_g}{\partial p}\right)+\left[\frac{\partial \vec{V}_g}{\partial x}\cdot\nabla\left(-\frac{\partial\phi}{\partial p}\right)\right]. \tag{6.34b}$$

Interestingly, $-\partial/\partial x$ of (6.35a) is equal to

$$\begin{aligned}
&-\frac{\partial}{\partial x}\left[\left(\frac{\partial}{\partial t}+\vec{V}_g\cdot\nabla\right)\left(-\frac{\partial\phi}{\partial p}\right)\right]\\
&=-\frac{\partial}{\partial x}\left[\frac{\partial}{\partial t}\left(-\frac{\partial\phi}{\partial p}\right)+u_g\frac{\partial}{\partial x}\left(-\frac{\partial\phi}{\partial p}\right)+v_g\frac{\partial}{\partial y}\left(-\frac{\partial\phi}{\partial p}\right)\right]\\
&=\left(\frac{\partial}{\partial t}+\vec{V}_g\cdot\nabla\right)\left(\frac{\partial^2\phi}{\partial x\partial p}\right)-\left[\frac{\partial\vec{V}_g}{\partial x}\cdot\nabla\left(-\frac{\partial\phi}{\partial p}\right)\right].
\end{aligned} \tag{6.35b}$$

Examination of the last lines of (6.34b) and (6.35b) proves that the geostrophic tendencies of $f_0\partial v_g/\partial p$ and $\partial^2\phi/\partial x\partial p$ (the two components of the thermal wind balance) have equal magnitude but opposite sign! Thus, the geostrophic wind destroys itself by changing the two parts of the thermal wind balance equally, but in opposite directions. Let us denote the magnitude of this geostrophic tendency as Q_1 so that

$$Q_1=-\frac{\partial\vec{V}_g}{\partial x}\cdot\nabla\left(-\frac{\partial\phi}{\partial p}\right).$$

If we now reinsert the ageostrophic terms that we previously neglected in developing (6.34a) and (6.35a), we get

$$f_0\frac{\partial}{\partial p}\left[\left(\frac{\partial}{\partial t}+\vec{V}_g\cdot\nabla\right)v_g+f_0u_{ag}\right]=\left(\frac{\partial}{\partial t}+\vec{V}_g\cdot\nabla\right)\left(f_0\frac{\partial v_g}{\partial p}\right)-Q_1+f_0^2\frac{\partial u_{ag}}{\partial p} \tag{6.36}$$

and

$$-\frac{\partial}{\partial x}\left[\left(\frac{\partial}{\partial t}+\vec{V}_g\cdot\nabla\right)\left(-\frac{\partial\phi}{\partial p}\right)-\sigma\omega\right]=\left(\frac{\partial}{\partial t}+\vec{V}_g\cdot\nabla\right)\left(\frac{\partial^2\phi}{\partial x\partial p}\right)+Q_1+\sigma\frac{\partial\omega}{\partial x}. \tag{6.37}$$

Multiplying (6.37) by −1 and adding it to (6.36) eliminates the time derivatives (since $f_0 \partial v_g / \partial p = \partial^2 \phi / \partial x \partial p$ by the thermal wind) and yields

$$-2Q_1 = \sigma \frac{\partial \omega}{\partial x} - f_0^2 \frac{\partial u_{ag}}{\partial p}. \tag{6.38}$$

The same set of operations can be performed on the x equation of motion and the thermodynamic energy equation resulting in

$$-2Q_2 = \sigma \frac{\partial \omega}{\partial y} - f_0^2 \frac{\partial v_{ag}}{\partial p} \tag{6.39}$$

where

$$Q_2 = -\frac{\partial \vec{V}_g}{\partial y} \cdot \nabla \left(-\frac{\partial \phi}{\partial p} \right).$$

Finally, taking $\partial / \partial x$ of (6.38) and adding it to $\partial / \partial y$ of (6.39) produces

$$-2\left(\frac{\partial Q_1}{\partial x} + \frac{\partial Q_2}{\partial y} \right) = \sigma \left(\frac{\partial^2 \omega}{\partial x^2} + \frac{\partial^2 \omega}{\partial y^2} \right) - f_0^2 \frac{\partial}{\partial p} \left(\frac{\partial u_{ag}}{\partial x} + \frac{\partial v_{ag}}{\partial y} \right)$$

which becomes, upon substituting from the continuity equation,

$$-2\left(\frac{\partial Q_1}{\partial x} + \frac{\partial Q_2}{\partial y} \right) = \sigma \left(\frac{\partial^2 \omega}{\partial x^2} + \frac{\partial^2 \omega}{\partial y^2} \right) + f_0^2 \frac{\partial^2 \omega}{\partial p^2} = \sigma \left(\nabla^2 + \frac{f_0^2}{\sigma} \frac{\partial^2}{\partial p^2} \right) \omega. \tag{6.40}$$

The RHS of (6.40) is identically the 3-D Laplacian operator found on the LHS of the classical quasi-geostrophic omega equation (6.26). The forcing function in this form of the quasi-geostrophic omega equation is given by twice the convergence of a 2-D horizontal vector quantity, the $\vec{Q}$-vector, defined as $\vec{Q} = (Q_1, Q_2)$ or

$$\vec{Q} = \left[\left(-\frac{\partial \vec{V}_g}{\partial x} \cdot \nabla \left(-\frac{\partial \phi}{\partial p} \right) \right) \hat{i}, \left(-\frac{\partial \vec{V}_g}{\partial y} \cdot \nabla \left(-\frac{\partial \phi}{\partial p} \right) \right) \hat{j} \right]. \tag{6.41}$$

Using the hydrostatic relationship ($\partial \phi / \partial p = -RT/p$) we can rewrite this expression in a more convenient form as

$$\vec{Q} = -\frac{R}{p} \left[\left(\frac{\partial \vec{V}_g}{\partial x} \cdot \nabla T \right) \hat{i}, \left(\frac{\partial \vec{V}_g}{\partial y} \cdot \nabla T \right) \hat{j} \right]$$

which is easier to employ with real weather maps. Looking again at (6.40), we see that if $\vec{Q}$ is convergent (divergent) then upward (downward) vertical motion results. Also, note that in deriving (6.40) there was no neglect of the deformation terms as we had been forced to do in prior derivations of an omega equation.

Now let us return to our original example of confluent flow superimposed upon a temperature gradient shown in Figure 6.8. The traditional approximations to the quasi-geostrophic omega equation might not be of much help in diagnosing omega in this environment since vorticity advection is rather difficult to determine here. The

completeness of the $\vec{Q}$-vector comes at the price of increased complication, however. Therefore, we examine the full expression of the $\vec{Q}$-vector in order to determine if a simplification, applicable to the example shown in Figure 6.8, is possible. The full expression of $\vec{Q}$ is given by

$$\vec{Q} = -\frac{R}{p}\left[\left(\frac{\partial u_g}{\partial x}\frac{\partial T}{\partial x} + \frac{\partial v_g}{\partial x}\frac{\partial T}{\partial y}\right)\hat{i} + \left(\frac{\partial u_g}{\partial y}\frac{\partial T}{\partial x} + \frac{\partial v_g}{\partial y}\frac{\partial T}{\partial y}\right)\hat{j}\right]. \tag{6.42}$$

But there is no $\partial T/\partial y$ in Figure 6.8 so, again employing the non-divergence of the geostrophic wind, $\vec{Q}$ simplifies to

$$\vec{Q} = -\frac{R}{p}\left[\left(\frac{\partial u_g}{\partial x}\frac{\partial T}{\partial x}\right)\hat{i} + \left(\frac{\partial u_g}{\partial y}\frac{\partial T}{\partial x}\right)\hat{j}\right] = -\frac{R}{p}\left(\frac{\partial T}{\partial x}\right)\left(\frac{-\partial v_g}{\partial y}\hat{i} + \frac{\partial u_g}{\partial y}\hat{j}\right)$$
$$= -\frac{R}{p}\left(\frac{\partial T}{\partial x}\right)\left[\hat{k}\times\frac{\partial \vec{V}_g}{\partial y}\right]. \tag{6.43}$$

So if one measures the change in the geostrophic wind vector along isotherms (i.e. along the y-axis), then the direction of the resulting $\vec{Q}$-vector is determined as the vertical cross-product of that vector change with its magnitude modulated by the intensity of the x-direction temperature gradient.

Figure 6.9(a) shows the $\vec{Q}$-vectors for the confluent jet entrance of Figure 6.8. This configuration of $\vec{Q}$-vectors results in $\vec{Q}$ convergence in the warm air and $\vec{Q}$ divergence in the cold air. Consequently, we have diagnosed a thermally direct, secondary, vertical circulation in which the warm air rises and the cold air sinks (Figure 6.9b). Such a secondary ageostrophic circulation achieves two important modifications of the environment. First, adiabatic cooling of the rising warm air and adiabatic warming of the sinking cold air decrease the magnitude of ∇T. This exactly counteracts the tendency of the geostrophic temperature advection in the confluent flow! Second, under the influence of the Coriolis force, the horizontal branches of this secondary ageostrophic circulation tend to increase the vertical wind shear – exactly counteracting the tendency of the geostrophic momentum advection in the confluent flow! Thus, the secondary ageostrophic circulation diagnosed with the $\vec{Q}$-vectors is precisely that necessary to restore the thermal wind balance in the face of the geostrophic wind's tendency to destroy the balance.

6.4.2 A natural coordinate version of the $\vec{Q}$-Vector

As we have just seen, the $\vec{Q}$-vector is a rather bulky expression but $-2\nabla\cdot\vec{Q}$ represents a complete form of the forcing in the quasi-geostrophic omega equation. Here we consider an expression for the $\vec{Q}$-vector distilled into a natural coordinate version

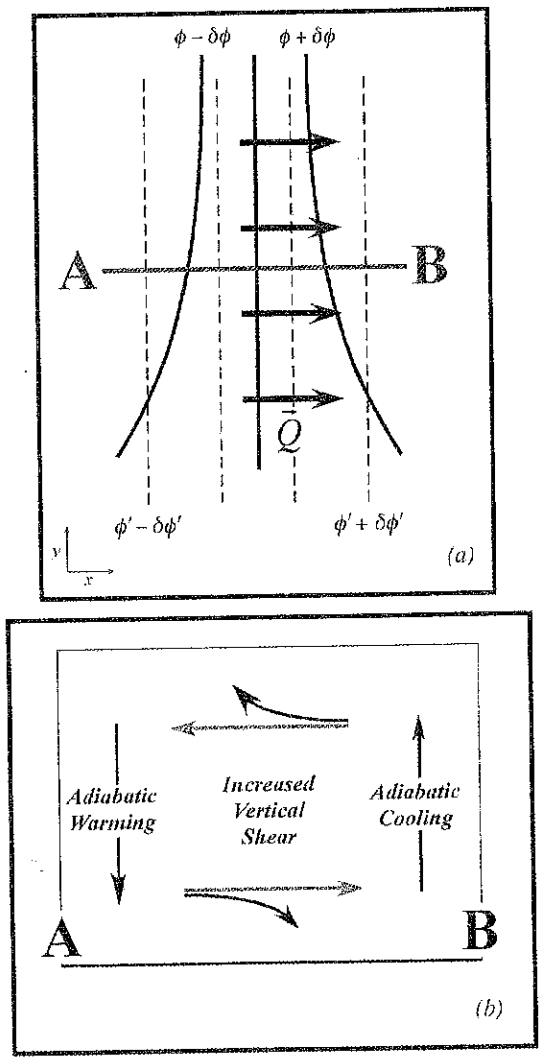

Figure 6.9 (a) $\vec{Q}$-vectors for the confluent jet entrance region depicted in Figure 6.8. Vertical cross-section along line A–B is shown in (b). (b) Vertical cross-section along line A–B in (a). Black arrows represent the vertical and horizontal branches of the secondary, ageostrophic circulation associated with the $\vec{Q}$-vector distribution in (a). Gray arrows represent the direction of the horizontal branch of the forced circulation before the *Coriolis* force turns in to the right. See text for explanation

that is easily applied to weather maps.[6] We begin with (6.42)

$$\vec{Q} = -\frac{R}{p}\left[\left(\frac{\partial u_g}{\partial x}\frac{\partial T}{\partial x} + \frac{\partial v_g}{\partial x}\frac{\partial T}{\partial y}\right)\hat{i} + \left(\frac{\partial u_g}{\partial y}\frac{\partial T}{\partial x} + \frac{\partial v_g}{\partial y}\frac{\partial T}{\partial y}\right)\hat{j}\right]$$

[6] This discussion follows work originally done by Sanders and Hoskins (1990).

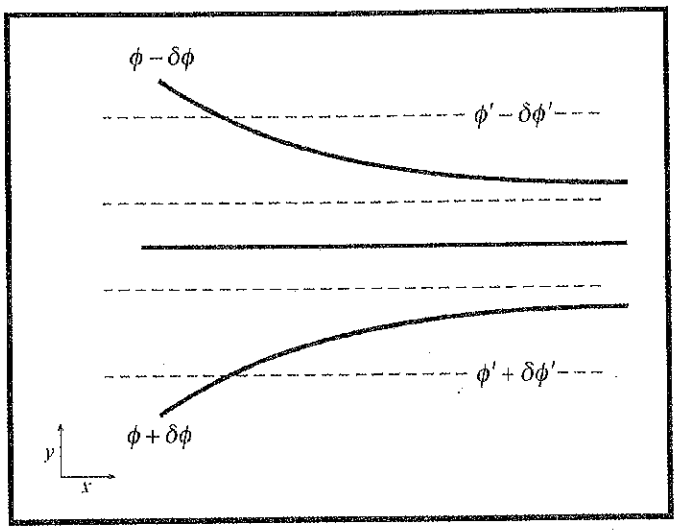

Figure 6.10 Zonally oriented, confluent jet entrance region in the northern hemisphere. Thick solid lines are 500 hPa geopotential height, dashed lines are 1000–500 hPa thickness. Note that for this flow configuration, $\partial T/\partial x = 0$

and consider, independently, two extreme examples in which $\partial T/\partial x = 0$ and $\partial T/\partial y = 0$. For the case of $\partial T/\partial x = 0$ we consider the confluent entrance region of a zonally oriented jet as in Figure 6.10. In such an environment, the above expression reduces to

$$\vec{Q} = -\frac{R}{p}\left(\frac{\partial T}{\partial y}\right)\left[\frac{\partial v_g}{\partial x}\hat{i} + \frac{\partial v_g}{\partial y}\hat{j}\right] = -\frac{R}{p}\left(\frac{\partial T}{\partial y}\right)\left[\frac{\partial v_g}{\partial x}\hat{i} - \frac{\partial u_g}{\partial x}\hat{j}\right]$$
$$= \frac{R}{p}\left(\frac{\partial T}{\partial y}\right)\left[\hat{k} \times \frac{\partial \vec{V}_g}{\partial x}\right]$$

since the geostrophic wind is non-divergent and

$$\frac{\partial v_g}{\partial x}\hat{i} - \frac{\partial u_g}{\partial x}\hat{j} = -\hat{k} \times \frac{\partial \vec{V}_g}{\partial x}.$$

Note that in this example, the x-axis is in the along-flow direction and the y-axis is in the across-flow direction, pointing toward colder air.

For the case of $\partial T/\partial y = 0$, we appeal to the confluent jet entrance in Figure 6.8 used to illustrate the utility of the $\vec{Q}$-vector. In that example, we found that the expression for $\vec{Q}$ reduced to

$$\vec{Q} = -\frac{R}{p}\left(\frac{\partial T}{\partial x}\right)\left[\hat{k} \times \frac{\partial \vec{V}_g}{\partial y}\right]$$

and the y-axis was in the along-flow direction with the x-axis in the across-flow direction pointing toward warmer air.

Let us now adopt natural coordinates $(\hat{s}, \hat{n})$ such that $\hat{s}$ is directed along the isotherms and $\hat{n}$ is directed across the isotherms toward warmer air. For the case of $\partial T/\partial x = 0$ (Figure 6.10) we could say that $\partial T/\partial y = -|\partial T/\partial n|$ (since $\partial T/\partial y < 0$). Analogously, we could say that $\partial \vec{V}_g/\partial x = \partial \vec{V}_g/\partial s$ so that our natural coordinate expression for $\vec{Q}$ would be

$$\vec{Q} = -\frac{R}{p}\left|\frac{\partial T}{\partial n}\right|\left[\hat{k} \times \frac{\partial \vec{V}_g}{\partial s}\right].$$

For the case of $\partial T/\partial y = 0$, we could say that $\partial T/\partial x = |\partial T/\partial n|$ (since $\partial T/\partial x > 0$). Also, we could say that $\partial \vec{V}_g/\partial y = \partial \vec{V}_g/\partial s$ so that our natural coordinate expression for $\vec{Q}$ would be, again,

$$\vec{Q} = -\frac{R}{p}\left|\frac{\partial T}{\partial n}\right|\left[\hat{k} \times \frac{\partial \vec{V}_g}{\partial s}\right], \tag{6.44}$$

demonstrating that this expression serves as the general natural coordinate expression for $\vec{Q}$. In order to apply this expression, we simply denote the vector change in the geostrophic wind along isotherms, take the vertical cross-product of that vector, and flip the resultant direction by 180° (as we must multiply by –1) to determine the direction of $\vec{Q}$. The magnitude is modulated by $|\partial T/\partial n|$.

Now we examine some examples for which the answers should be fairly familiar. First, let us consider a pattern of sea-level isobars and isotherms for an idealized train of cyclones and anticyclones, illustrated in Figure 6.11. Choosing the middle isotherm as our $\hat{s}$-axis, we need only consider the vector change in the geostrophic wind along *that* isotherm. Upon doing so we find that the $\vec{Q}$-vectors converge to the east of the sea-level low-pressure center and diverge to its west. Thus, we have diagnosed ascent to the east of the cyclone and descent to the east of the anticyclone.

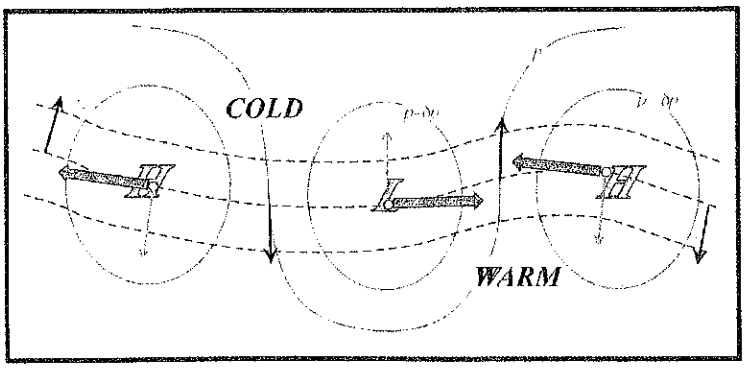

Figure 6.11 Schematic train of lows and highs in the northern hemisphere. Thin solid lines are sea-level isobars, black dashed lines are 1000–500 hPa thickness, black arrows are surface geostrophic winds, light gray arrows represent $\partial \vec{V}_g/\partial s$, and shaded arrows are $\vec{Q}$-vectors. See text for explanation

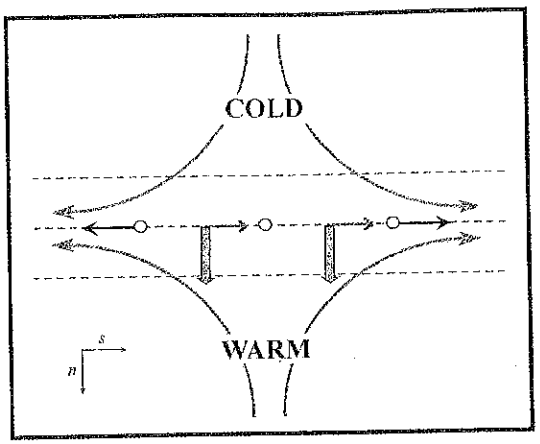

Figure 6.12 Isotherms in a region of geostrophic deformation. Curved gray arrows are geostrophic streamlines, dashed lines are isotherms or thickness isopleths, black arrows are geostrophic winds at the indicated circles. This gray arrows represent $\partial \vec{V}_g/\partial s$, and the shaded gray arrows are the $\vec{Q}$-vectors

In this way, the train of cyclones and anticyclones propagates to the east, in the direction of the thermal wind – a result we noted earlier in the chapter.

Next we consider a zonally oriented bundle of isentropes placed in a region of pure geostrophic deformation as illustrated in Figure 6.12. Clearly, this environment would not be easily diagnosed using the traditional form of the quasi-geostrophic omega equation nor any of the approximations to it that we have examined. Picking the middle isotherm as the $\hat{s}$-axis, we need only consider the geostrophic wind variation along that isotherm. The resulting $\vec{Q}$-vectors are uniformly pointed toward the warm side of the baroclinic zone, indicating rising warm air and sinking cold air – a thermally direct vertical circulation. The differential thermal advection occurring in this deformation zone would tend to bring the isotherms closer together in the horizontal, thereby increasing the thermal wind shear. This same underlying dynamical principle was discussed in reference to Figure 6.4(b). In the next chapter we will more fully discuss the relationship between changes in the temperature gradient and attendant vertical circulations as we discuss frontogenesis. Finally we consider a hypothetical field of uniform geostrophic temperature advection as depicted in Figure 6.13. It is easy to demonstrate that since there is no variation of the geostrophic wind along any isotherm, there is no $\vec{Q}$-vector field and, hence, no quasi-geostrophic vertical motion.

We have said that the $\vec{Q}$-vector form of the quasi-geostrophic omega equation is a complete form of the forcing. This distinguishes it from the Sutcliffe and Trenberth approximations wherein the deformation terms are neglected. Two reasonable questions to ask at this point in our discussion are (1) where are the deformation terms hiding in the $\vec{Q}$–vector forcing, and (2) are they really negligible? The first question is rather academic but the second is crucially important to operational forecasting.

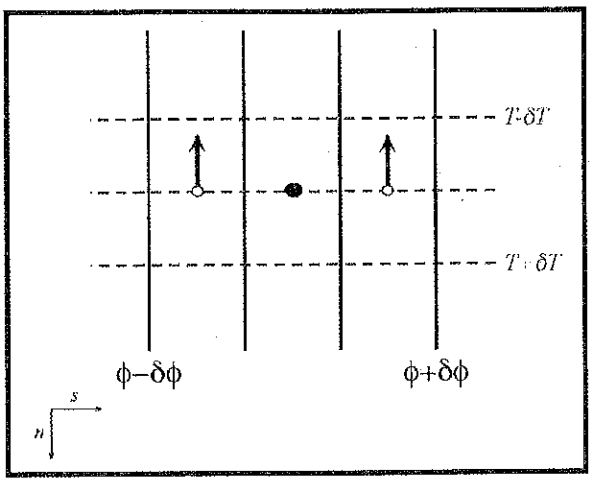

Figure 6.13 Geopotential heights (thick black lines) and isotherms (dashed lines) in a field of uniform geostrophic warm air advection. Arrows are the geostrophic winds at the indicated points. Since the geostrophic flow is uniform, $\partial \vec{V}_g/\partial s$ is zero at the black dot and hence there is no $\vec{Q}$-vector and no $\vec{Q}$-vector divergence

Recall that the forcing for ω in the $\vec{Q}$-vector form of the quasi-geostrophic omega equation is given by

$$Forcing \;=\; -2\nabla \cdot \vec{Q} = -2\left(\frac{\partial Q_1}{\partial x} + \frac{\partial Q_2}{\partial y}\right). \tag{6.45}$$

Using (6.42), this can be written as

$$Forcing = -2\frac{R}{p}\left[\frac{\partial}{\partial x}\left(-\frac{\partial \vec{V}_g}{\partial x}\cdot\nabla T\right) + \frac{\partial}{\partial y}\left(-\frac{\partial \vec{V}_g}{\partial y}\cdot\nabla T\right)\right]$$

which expands to four terms after applying the chain rule to yield

$$Forcing = -2\frac{R}{p}\left\{\left[\frac{\partial}{\partial x}\left(-\frac{\partial \vec{V}_g}{\partial x}\right)\cdot\nabla T + \frac{\partial}{\partial y}\left(-\frac{\partial \vec{V}_g}{\partial y}\right)\cdot\nabla T\right] + \left[-\frac{\partial \vec{V}_g}{\partial x}\cdot\nabla\frac{\partial T}{\partial x} - \frac{\partial \vec{V}_g}{\partial y}\cdot\nabla\frac{\partial T}{\partial y}\right]\right\}. \tag{6.46}$$

It is left as an exercise to the reader to show that the first square bracketed term on the RHS of (6.46) is exactly equal to the Sutcliffe/Trenberth approximation to the forcing function of the quasi-geostrophic omega equation. Of course, that means that the second square bracketed term on the RHS of (6.46) represents the oft neglected deformation terms. As pointed out previously, these terms will be significant any time a second derivative of temperature is coincident with a first derivative of the geostrophic wind. Frontal zones fit this description but many other characteristic thermal structures observed in mid-latitude cyclones do as well. Figure 6.14

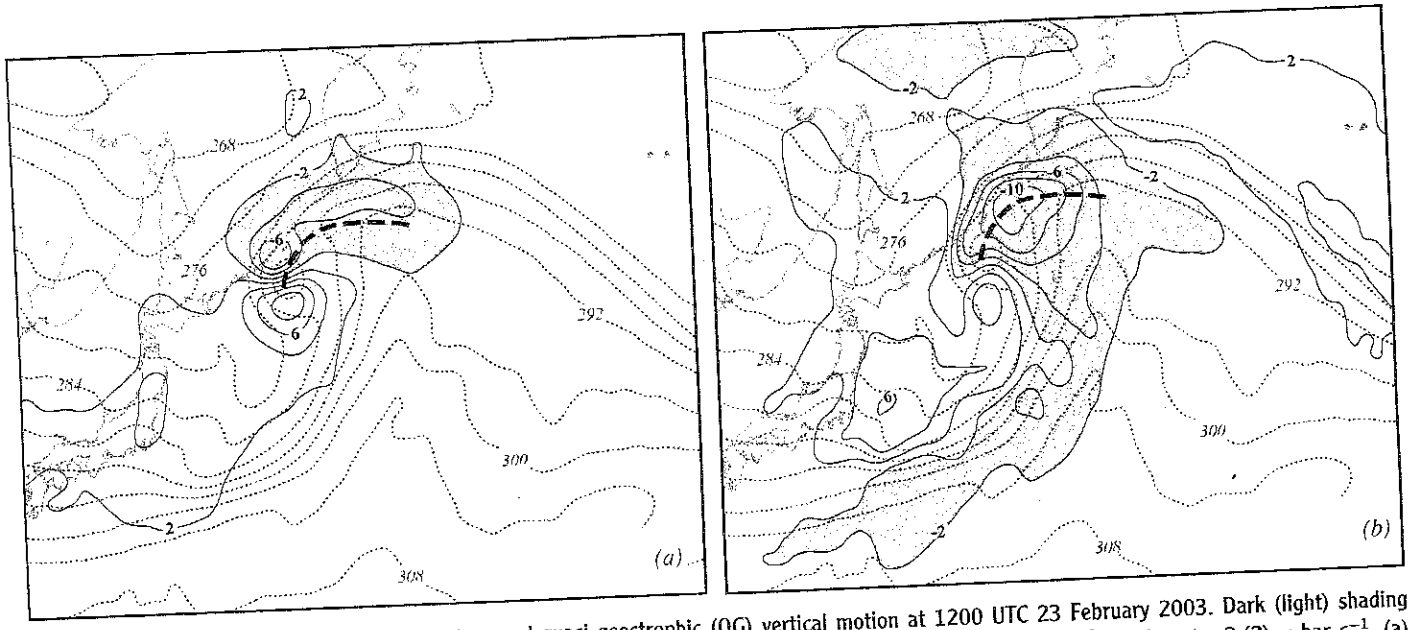

Figure 6.14 The 700 hPa potential temperature and quasi-geostrophic (QG) vertical motion at 1200 UTC 23 February 2003. Dark (light) shading represents upward (downward) vertical motion labeled in μ bar s^{-1} (dPa s^{-1}) and contoured every -2 (2) μ bar s^{-1} starting at -2 (2) μ bar s^{-1}. (a) Sutcliffe/Trenberth approximation to the QG vertical motion. (b) The deformation term contribution to the QG vertical motion. In both panels the thick, dashed line is the axis of the occluded thermal ridge

illustrates the quasi-geostrophic (QG) omega resulting from both the Sutcliffe/Trenberth forcing terms (Figure 6.14a) and the deformation terms (Figure 6.14b) for a modest occluded cyclone. Note that the occluded thermal ridge, a non-frontal thermal structure, is the seat of significant QG vertical motions associated with the deformation terms. This ascent would not be accounted for in the Sutcliffe/Trenberth approximation to the QG omega equation.

6.4.3 The along- and across-isentrope components of $\vec{Q}$

A final word concerning the physical meaning of the $\vec{Q}$-vector is appropriate before we begin to discuss frontogenesis in Chapter 7. This comment begins by rewriting the hydrostatic equation in the form $-\partial\phi/\partial p = f\gamma\theta$ where θ is the potential temperature and γ is a constant on isobaric surfaces, i.e.

$$\gamma = \frac{R}{fp_0}\left(\frac{p_0}{p}\right)^{c_v/c_p},$$

with p_0 usually taken to be 1000 hPa. Employing this form of the hydrostatic equation allows (6.41) to be rewritten as

$$\vec{Q} = f\gamma\left[\left(-\frac{\partial \vec{V}_g}{\partial x}\cdot\nabla\theta\right)\hat{i}, \left(-\frac{\partial \vec{V}_g}{\partial y}\cdot\nabla\theta\right)\hat{j}\right]. \tag{6.47}$$

Now let us consider the Lagrangian rate of change of $\nabla\theta$ following the geostrophic flow, in symbols,

$$\frac{d}{dt_g}\nabla\theta = \left(\frac{\partial}{\partial t} + \vec{V}_g\cdot\nabla\right)\nabla\theta = \left(\frac{\partial}{\partial t} + \vec{V}_g\cdot\nabla\right)\left(\frac{\partial\theta}{\partial x}\hat{i} + \frac{\partial\theta}{\partial y}\hat{j}\right). \tag{6.48}$$

It is left to the reader to show that, under adiabatic conditions,

$$f\gamma\frac{d}{dt_g}\nabla\theta = \vec{Q}.$$

Thus, a profound physical meaning can be ascribed to the $\vec{Q}$-vector: that is, $\vec{Q}$ *describes the rate of change of* $\nabla\theta$ *following the geostrophic flow.* This property of the $\vec{Q}$-vector will be exploited in our subsequent discussions of both frontogenesis and cyclogenesis. For now, it is enough that we take advantage of this physical fact to develop additional insight from the $\vec{Q}$-vector.

Given that

$$\vec{Q} = f\gamma\frac{d}{dt_g}\nabla\theta,$$

it is useful to consider separately the along- and across-isentrope components of $\vec{Q}$, denoted as $\vec{Q}_s$ and $\vec{Q}_n$ (where $\vec{Q} = \vec{Q}_s + \vec{Q}_n$), respectively, illustrated in schematic form in Figure 6.15. Before deriving mathematical expressions corresponding to $\vec{Q}_s$

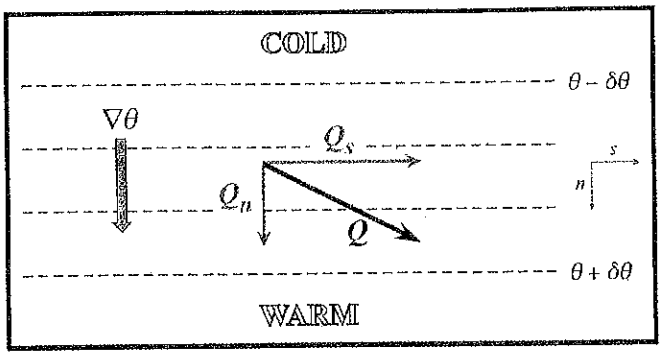

Figure 6.15 Natural coordinate partition of the $\vec{Q}$-vector into its along-isentrope ($\vec{Q}_s$) and across-isentrope ($\vec{Q}_n$) components. See text for explanation

and $\vec{Q}_n$, let us consider their respective physical meanings. Noting that the vector $\nabla\theta$, like all vectors, has both magnitude and direction, it is clear that $\vec{Q}_n$, which is directed along $\nabla\theta$, can only affect changes in the *magnitude* of $\nabla\theta$. Since $\vec{Q}_s$ is directed perpendicularly to $\nabla\theta$ it can only affect changes in the *direction* of $\nabla\theta$. Now, $\vec{Q}_n$ is simply the component of $\vec{Q}$ along the vector $\nabla\theta$ and simple vector calculus yields a mathematical expression for $\vec{Q}_n$ as

$$\vec{Q}_n = \left(\frac{\vec{Q}\cdot\nabla\theta}{|\nabla\theta|}\right)\frac{\nabla\theta}{|\nabla\theta|}. \tag{6.49}$$

Allowing the unit vector in the $\nabla\theta$ direction ($\nabla\theta/|\nabla\theta|$) to be written as $\hat{n}$, and the magnitude of $\vec{Q}_n$ ($\vec{Q}\cdot\nabla\theta/|\nabla\theta|$) to be written as Q_n, (6.49) can be rewritten as $\vec{Q}_n = Q_n\hat{n}$. Similarly, $\vec{Q}_s$ is the component of $\vec{Q}$ along the vector $\hat{k}\times\nabla\theta$ and so can be written as

$$\vec{Q}_s = \left[\frac{\vec{Q}\cdot(\hat{k}\times\nabla\theta)}{|\nabla\theta|}\right]\frac{\hat{k}\times\nabla\theta}{|\nabla\theta|} \tag{6.50}$$

where we have taken advantage of the fact that $|\hat{k}\times\nabla\theta| = |\nabla\theta|$. Allowing the unit vector in the $\hat{k}\times\nabla\theta$ direction to be denoted as $\hat{s}$ and the magnitude of $\vec{Q}_s$ ($\vec{Q}\cdot(\hat{k}\times\nabla\theta)/|\nabla\theta|$) to be denoted as Q_s, (6.50) can be written as $\vec{Q}_s = Q_s\hat{s}$. Substituting the expressions for both $\vec{Q}_n$ and $\vec{Q}_s$, we can write

$$\vec{Q} = Q_n\hat{n} + Q_s\hat{s}. \tag{6.51}$$

Since the total QG vertical motion is related to $-2\nabla\cdot\vec{Q}$, the foregoing partition allows us to see that total as the sum of two orthogonal parts associated with $-2\nabla\cdot\vec{Q}_n$ and $-2\nabla\cdot\vec{Q}_s$, respectively. Given the orientations of $\vec{Q}_n$ and $\vec{Q}_s$, these components of the total vertical motion will be distributed in couplets across the thermal wind (transverse) and along the thermal wind (shearwise), respectively.

It will be shown in the next chapter that the transverse component of the QG omega is directly related to the dynamics of the frontal zones that characterize the

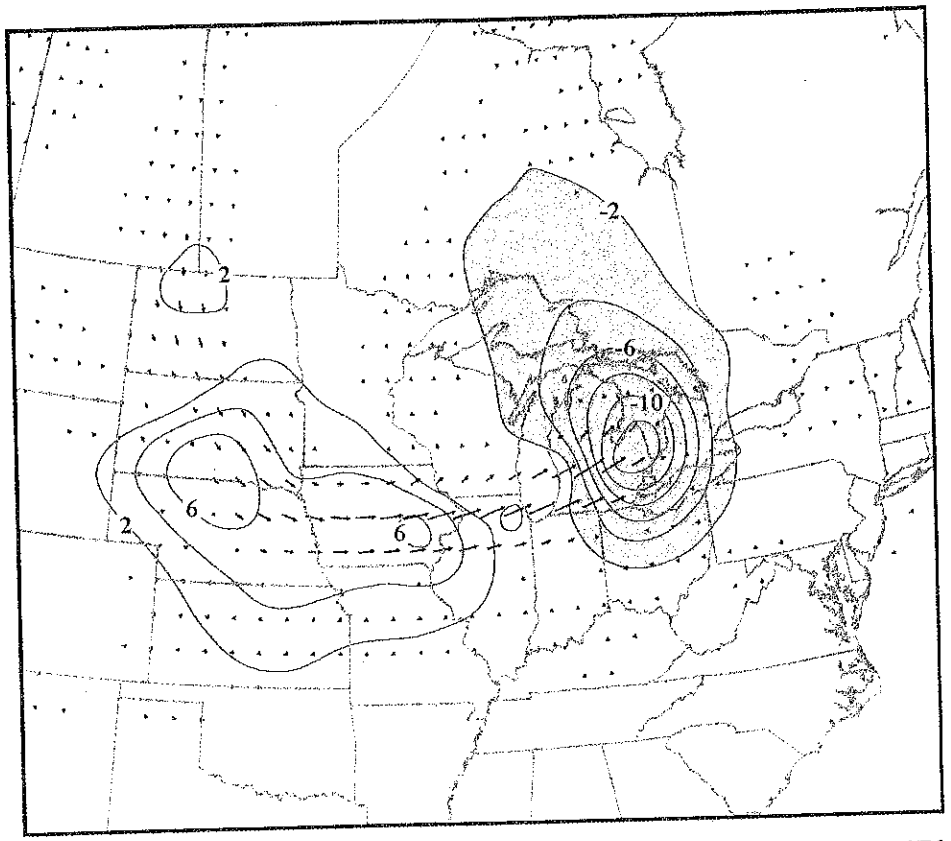

Figure 6.16 The 700 hPa $\vec{Q}_{T_R}$ vectors (black arrows) and associated QG vertical motion at 0000 UTC 13 November 2003. Vertical motion shown in units of μ bar s^{-1} (dPa s^{-1}) contoured every 2μ bar s^{-1} with dark shading showing upward vertical motions and light shading showing downward vertical motion

mid-latitude cyclone. Insight into the nature of the shearwise component arises by considering an alternative form of the Trenberth approximation to the QG omega equation in which the thermal wind advection of geostrophic absolute vorticity was the principal forcing mechanism for vertical motions. Starting with (6.32)

$$\sigma\left(\nabla^2 + \frac{f_0^2}{\sigma}\frac{\partial^2}{\partial p^2}\right)\omega \approx 2\left[f_0\frac{\partial \vec{V}_g}{\partial p}\cdot\nabla(\zeta_g + f)\right]$$

and taking advantage of the non-divergence of the geostrophic wind while neglecting the contribution of the planetary vorticity to the geostrophic absolute vorticity, we note that the RHS can be written in a flux divergence form as

$$\sigma\left(\nabla^2 + \frac{f_0^2}{\sigma}\frac{\partial^2}{\partial p^2}\right)\omega \approx 2\nabla\cdot\left[f_0\frac{\partial \vec{V}_g}{\partial p}\zeta_g\right]. \qquad (6.52a)$$

But since

$$\frac{\partial \vec{V}_g}{\partial p} = \frac{\hat{k}}{f} \times \nabla \frac{\partial \phi}{\partial p} = -\gamma(\hat{k} \times \nabla\theta),$$

(6.52a) can be rewritten as

$$\sigma \left(\nabla^2 + \frac{f_0^2}{\sigma} \frac{\partial^2}{\partial p^2} \right) \omega \approx -2\nabla \cdot \vec{Q}_{TR} \tag{6.52b}$$

where $\vec{Q}_{TR} = f_0 \gamma \zeta_g (\hat{k} \times \nabla\theta)$. Thus, the approximate Trenberth form of the QG omega equation can be written in a form that is identical to the $\vec{Q}$-vector form of the full omega equation. Note that the vector $\vec{Q}_{TR}$ must be everywhere parallel to isentropes and thus $\vec{Q}_{TR}$ represents at least a portion of $\vec{Q}_s$.[7] An illustration of the distribution of $\vec{Q}_{TR}$ vectors and the associated QG vertical motions from the developing cyclone previously examined in Figure 6.6 are illustrated in Figure 6.16. The distinction between such shearwise and transverse vertical motions will prove valuable when we discuss the process of mid-latitude cyclogenesis in Chapter 8.

Selected References

Sutcliffe (1939) offers an illuminating discussion of the ageostrophic wind and its role in producing vertical motions.

Sutcliffe (1947) describes his famous development theorem.

Trenberth (1978) describes the cancellation among terms in the traditional QG omega equation.

Hoskins *et al.* (1978) provide the seminal derivation and discussion of the $\vec{Q}$-vector.

Martin (1998b) examines the appropriateness of neglecting the deformation terms in the QG omega equation from the perspective of the $\vec{Q}$-vector.

Problems

6.1. (a) For the mid-latitude, upper tropospheric wave train shown in Figure 6.1A, indicate where the regions of ascent and descent are found. Explain your answer.

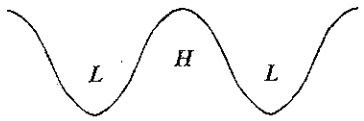

Figure 6.1A

[7] A full description of both the $\vec{Q}_n$ and $\vec{Q}_s$ components of the $\vec{Q}$-vector, along with their application to the diagnosis of vertical motions in the occluded quadrant of mid-latitude cyclones, is given in Martin (1999).